ECCOMAS Congress 2016
VII European Congress on Computational Methods in Applied Sciences and Engineering
M. Papadrakakis, V. Papadopoulos, G. Stefanou, V. Plevris (eds.)
Crete Island, Greece, 5–10 June 2016

EXPERIMENTAL VALIDATION OF COMPOSITE STRUCTURES IN EXPLICIT IMPACT ANALYSIS

Konstantinos T. Fotopoulos[1], **George N. Lampeas**[2]

Laboratory of Technology and Strength of Materials
Department of Mechanical Engineering and Aeronautics
University of Patras, 26500 Rion, Greece
[1] fotopk@mech.upatras.gr
[2] labeas@mech.upatras.gr

Keywords: Model Validation, Composite laminate, Low velocity impact, Finite element analysis, Delamination, Stacked shell modeling.

Abstract. *The prediction of composite laminate behavior when subjected to low velocity impact loading is a challenging task due to the complexity of the fully three dimensional stress state that develops inside the structure. Several methods have been employed in order to analyze the intralaminar and interlaminar failure modes that evolve during impact. In the present work a stacked shell methodology is proposed for the simulation of composite laminates. The approach is experimentally validated through the comparison of its results to the respective of a low velocity impact on laminated specimens test. The numerical predictions correlate well to the experimental results, showing the accuracy of the stacked-shell approach in explicit impact analysis of composite structures.*

1 INTRODUCTION

Lightweight structural design has become very important in the automotive, marine and aircraft engineering fields. The increasing demand for materials that combine low weight with high mechanical strength has generated high interest in the analysis of the behavior of composite materials. One of the most significant issues of this analysis is the effect of impact loading on composite laminated structures, especially because of their susceptibility to out-of-plane failure. Although a wide range of scenarios exist, impact on composites can generally be categorized in low and high velocity impact. The former usually includes cases of projectiles with significant mass and volume that are dropped on the structure, while the latter mostly comprises instances of small projectiles impacting composites at high speeds. The effects of such impact events on a laminate include fiber failure, matrix cracks as well as separation of plies (delamination); hence, the outcome consists of a combination of failure modes making the analysis of the impact response a demanding task.

In order to accurately simulate the different phenomena arising during an impact event, several predictive methods has been utilized. The main approaches for the numerical simulation of impact induced effects are based on Continuum Damage Mechanics (CDM) and Fracture Mechanics. In CDM material models [1-3] both the plies and the interfaces of a composite are modeled using appropriate damage theories. On the other hand, fracture mechanics techniques – e.g. the Virtual Crack Closure Technique (VCCT) or the Cohesive Zone Method (CZM) – treat in-plane and out-of-plane behavior separately, concentrating individually on the progression of interlaminar damage [4]. The VCCT [5] has been applied extensively in the analysis of metals and has been extended to composite materials using the energy release rate concepts to directly predict the crack growth. However, the location and size of the crack are prerequisites for the application of the method, making it difficult to be employed in more complex structures. The CZM – based on the works of Dugdale [6] and Barenblatt [7] – assumes that a cohesive zone is developed in front of the crack tip, with the cohesive surfaces associated with the crack being connected by cohesive laws. This technique is capable of predicting separation growth without the assumptions of the VCCT, although it presents a certain degree of mesh dependency.

Considering laminated composites as a conjunction of fiber reinforced plies and matrix interfaces, the analysis of a composite's behavior can be approached in the Finite Element (FE) environment using CDM techniques to address intralaminar failure and Fracture Mechanics techniques to simulate interlaminar failure. In this frame, the representation of out-of-plane normal and shear deformation through-thickness can be achieved by stacking an appropriate number of 2D damage mechanics elements through the laminate thickness, held together by cohesive traction. This approach is mentioned in the literature as 'stacked shell' or 2.5D approach. It is based on the CDM approach proposed by Allix and Ladeveze [1], replacing the CDM matrix representation with cohesive zone interfaces. The main advantage of this modeling technique is the revocation of aspect ratio restrictions concerning the in-plane and through thickness element dimensions, presenting obvious advantages in regard to simulation accuracy and computational efficiency, compared to traditional modeling techniques. In the studies [8-14] of the literature the use of the stacked shell method has been reported for the simulation of composite laminates.

The aim of the present work is the study of the appropriateness of the stacked shell approach capabilities in explicit analysis of low velocity impact events, as well as in the prediction of interlaminar damage initiation and growth. The accuracy of the stacked shell modeling technique is assessed by an experimental procedure, concerning low velocity impact on com-

posite laminates. Numerical predictions are compared to published experimental data, derived from Ultrasound A-scan, Ultrasound C-scan and Thermography non-destructive tests.

2 DESCRIPTION OF THE MODELLING APPROACH

The stress distribution produced by impact on a laminated composite is three-dimensional. Complex phenomena that include propagation of compressive, shear and surface stress waves occur during the impact event [15]. The simulation of the stress state that develops under these conditions is a challenging task, which requires a modeling strategy which is capable to predict the three-dimensional stress state of the laminate.

The idea behind the stacked shell FE model development is based on the hypothesis that a composite laminate can be simulated by a number of discrete sublaminates which are kinematically tied by cohesive interfaces simulating the matrix. In this manner, the sublaminates are mainly burdened with the axial and bending loads which are developed in the laminate, while the cohesive interfaces take into account the out-of-plane normal and shear loading effects. In this way the displacement and strain continuity between adjacent sublaminates is provided, since forces are transferred from one sublaminate to another through the cohesive interfaces. Accordingly, the FE modeling strategy can be divided in:

a) In-plane damage modeling

b) Interface modeling

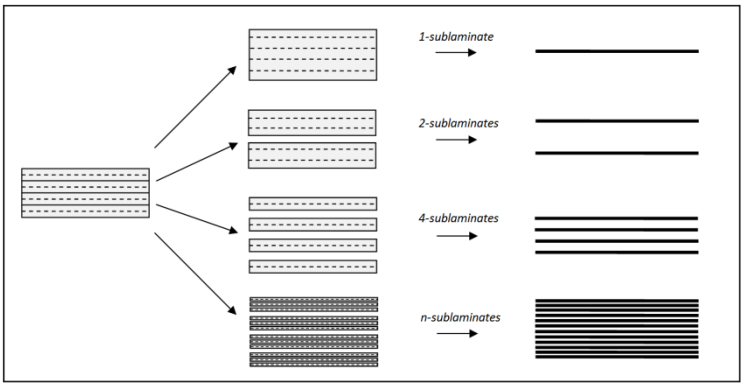

Figure 1: Representation of the stacked shell approach (taken from [14])

2.1 In-plane damage modeling

The low velocity impact induced in-plane damage mainly consists of fiber failure and matrix cracking. The simulation of these failure modes is performed through the use of a CDM elastic-plastic material model which is based on the concept of failure surfaces. The longitudinal, transverse and shear strengths are taken for the yield function, resulting to a faceted surface. The failure surfaces for this material model are:

$$\begin{aligned} \sigma_{1t} &= aX_t \\ \sigma_{1c} &= -X_c \\ \sigma_{2t} &= aY_t \\ \sigma_{2c} &= -Y_c \\ \sigma_{12} = \sigma_{23} &= \sigma_{13} = \pm S_c \end{aligned} \tag{1}$$

where σ_{1t}, σ_{1c}, σ_{2t}, σ_{2c}, σ_{12}, σ_{23}, σ_{13} are the stresses expressed in the material principal axes (1 for the axial fiber direction, 2 for the transverse matrix direction and 3 for the through-thickness direction) X_t, X_c are the longitudinal tensile and compressive strengths, respectively, Y_t, Y_c are the transverse tensile and compressive strengths, respectively and S_c is the in-plane shear strength. The parameter a can be used to limit the tensile failure, when the respective strengths have been reached. For a = 1 the material model results in a fully elastic-plastic model that retains the initially defined strength values for the failure surface. For a = 0, the tensile stresses σ_{1t} and σ_{2t} are reduced to zero after strengths X_t, Y_t have been reached; subsequently, only compressive and shear loads can be carried.

According to a work performed by Maimi et al [16], in order to ensure the correct calculation of dissipated energy independently of the element size, the elastic energy of an element during damage initiation must be lower than or equal to the fracture energy. Therefore, the material strengths used in the material model for each damage law have to be modified, using Equation 2.

$$X_M = \sqrt{\frac{2E_M G_M}{l^*}} \tag{2}$$

where X, E are the strengths and moduli of the material respectively, in the direction denoted by the subscript M (longitudinal, transverse or shear), l^* is the element characteristic length and G_M is the fracture toughness. The characteristic length of square elements for unknown direction of crack propagation can be approximated as proposed by Bazant and Oh [17] by

$$l^* = \frac{\sqrt{A_{IP}}}{\cos(\gamma)} \tag{3}$$

where γ is the angle that the mesh lines and the crack direction form and A_{IP} is the area corresponding to an integration point. If the direction of crack propagation is unknown, the average of Equation 3 can be used:

$$l^* = 1.12\sqrt{A_{IP}} \tag{4}$$

Consequently, the effect of element size to the material model for in-plane damage is minimized.

2.2 Interface modeling – cohesive zone method

The damage that the interfaces of a laminate undergo during impact events constitutes of de-bonding between adjacent plies, i.e. delamination. Modeling of interface failure is realized through the implementation of a fracture mechanics based approach, which is a combination of a cohesive zone model and a linear elastic adhesive penalty formulation as proposed by Borg [18].

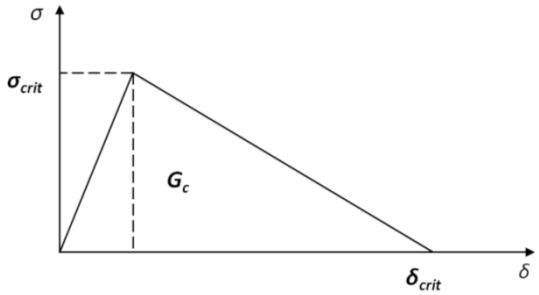

Figure 2: Cohesive law - Traction-separation curve

Regions between sublaminates are introduced through which damage initiation and growth is possible. In particular, the constitutive behavior of the cohesive surfaces is described by a bilinear law, as shown in Figure 2. The interface damage initiates when the failure criterion of Equation 5 is met.

$$\left(\frac{|\sigma_n|}{\sigma_{n,crit}}\right)^2+\left(\frac{|\sigma_s|}{\sigma_{s,crit}}\right)^2\geq 1 \tag{5}$$

In the above equation σ_n, σ_s are the normal and shear stresses respectively and $\sigma_{n,crit}$, $\sigma_{s,crit}$ are the failure stresses that correspond to each component. After the failure initiation point, damage between cohesive surfaces is a linear function of the distance between them. When the distance δ_{crit} is reached, the cohesive surfaces are released and complete ply separation occurs.

The length of the cohesive zone created at the tip of a crack is the distance from the crack tip to the point of maximum cohesive traction. According to Turon et al [19] the constitutive parameters for the simulation of delamination can be determined in order to adapt the length of the cohesive zone to the element size so that the energy dissipation is correct. This is performed using Equation 6.

$$\sigma_{crit}=\sqrt{\frac{9\pi EG_c}{32N_e l_e}} \tag{6}$$

where E is the transverse modulus of elasticity, G_c is the critical energy release rate, N_e is the number of elements in the cohesive zone and l_e is the element length in the crack propagation direction. The interface failure stress is then selected as the minimum between the value calculated by Equation 6 and the nominal failure stress. The regularization of the stress by Equation 6 ensures that the interface model will remain practically unaffected by mesh size produced artificial phenomena.

3 EXPERIMENTAL VALIDATION OF THE IMPACT SIMULATIONS

The capabilities of the stacked shell approach with respect to the prediction of the behavior of composite laminates are assessed through comparison of simulation results to the experimental results of a low velocity impact drop test.

3.1 Description of the experimental procedure

The experimental procedure has been performed by Riccio et al [20] according to the European association of Aerospace Manufacturers standard prEN 6038. The experiment involves the impact of a hemispherical impactor on a laminated plate with rectangular geometry, fabricated by the G1157/RTM-6 material system. The plate consists of 8 plies of 0.3 mm thickness each, resulting to a $[0/90/45/-45]_s$ layup. The dimensions of the flat specimen are 150 mm × 100 mm × 2.4 mm (Length × Width × thickness). The impactor's radius is 8 mm, with a mass of 3.64 kg. The specimen is supported by a fixture frame with a 125 mm × 75 mm rectangular window and is constrained by 4 rigid clamps with 10 mm diameter and 3 mm height. Impact on the plate is performed for three energy levels, namely 6 J, 10 J and 13J. Results are acquired by Ultrasound A-scan, Ultrasound C-scan and Thermography non-destructive tests.

3.2 FE model development

The FE model was developed in the explicit code of LS-Dyna, according to the simulation approach described in Section 2. It comprises eight sublaminates, each one representing a layer of the laminated plate, as shown in Figure 3. The sublaminates are modeled by fully integrated Reissner-Mindlin shell elements with six degrees of freedom per node, i.e. three translations (u*x*, u*y*, uz) and three rotations (rot*x*, rot*y*, rotz). This element type presents a Bathe-Dvorkin [21] transverse shear treatment in order to eliminate w-hourglass modes, while other hourglass modes are eliminated by selectively reduced integration. In the LS-Dyna environment this behavior is included in shell element formulation 16 [22].

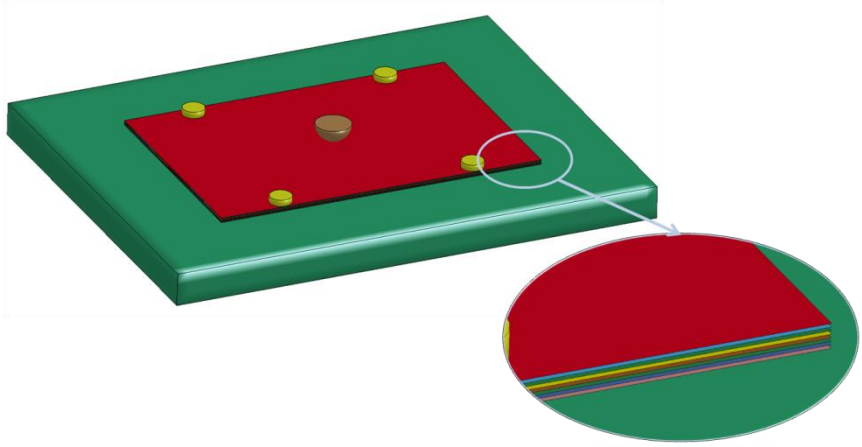

Figure 3: Finite element model of the low velocity impact test

Following a mesh convergence parametric investigation, each sublaminate is discretized by a finite element mesh consisting of 2 mm x 2 mm square elements and four integration points through-thickness. Equation 2 is used to modify material strengths in order to correspond to the element characteristic length, calculated by Equation 4. The G1157/RTM-6 lamina material properties as well as the intralaminar damage parameters (Table 1) that are used for the simulation of sublaminates are introduced in the 'Mat 59 Composite Failure' type of the LS-Dyna code, which is formulated according to the attributes of the elasto-plastic material model described in section 2.1.

G1157/RTM-6 Material Properties	ρ [kg/m^3]	E_a [GPa]	$E_b=E_c$ [GPa]	$G_{ab}=G_{ca}=G_{bc}$ [GPa]	$\nu_{ab}=\nu_{ac}=\nu_{bc}$
	1400	130.05	11.55	6.0	0.312
G1157/RTM-6 In-plane fracture energies	GF_{ftc} [kJ/m^2]	GF_{fcc} [kJ/m^2]	GF_{mtc} [kJ/m^2]	GF_{mcc} [kJ/m^2]	
	16.4	5.9	0.5	4.62	
G1157/RTM-6 Ply Damage Parameters	**Longitudinal Tensile Strength** [MPa]	**Longitudinal Compressive Strength** [MPa]	**Transverse Tensile Strength** [MPa]	**Transverse Compressive Strength** [MPa]	**In-plane Shear Strength** [MPa]
	1380	827.7	71.8	218.3	90

Table 1: G1157/RTM-6 Material properties and damage parameters

Regarding the FE implementation of interfaces, seven inter-layers were introduced between sublaminates. A tiebreak contact formulation is selected for the simulation of interlaminar behaviour. When the defined critical distance between initially tied nodes is reached, the tiebreak contact is released and converted to a typical surface-to-surface contact. According to Dobyns [23], delamination growth occurs because of transverse shear stresses developed at the area of impact. For this reason, Equation 6 is used to calculate the shear failure stress, with element length l_e equal to 2 mm and the desired number of elements in the cohesive zone N_e is set equal to 5, which was shown to produce accurate results [19]. Subsequently, the critical release distance δ_{crit} can be calculated using known values of the shear energy release rate which is approximated by Equation 7. Finally, the calculated value of the critical distance is substituted in Equation 8 that approximates the normal energy release rate in order to determine the normal failure stress. The interlaminar damage parameters, shown in Table 2, are defined in Option 8 of the 'Contact automatic one way surface to surface tiebreak' type, which is based on the CZM model presented in section 2.2.

$$G_{IIC} = \frac{1}{2}\sigma_{s,crit}\delta_{crit} \tag{7}$$

$$G_{IC} = \frac{1}{2}\sigma_{n,crit}\delta_{crit} \tag{8}$$

The impactor, fixture base and clamps are discretized with a relatively coarse mesh using three-dimensional solid elements, and their geometry is assumed to remain undeformed during the impact event. For this reason they are modeled using 'Mat 020 Rigid' of the LS-Dyna code. All degrees of freedom of the fixture base and clamps are constrained, while for the rigid impactor, only movement in the direction normal to the target surface is allowed. A typical penalty based surface to surface contact algorithm is used between the impactor, laminated plate and fixture base. To simulate the interaction between rigid clamps and the specimen, a penalty-based tied contact is used ('Contact tied surface to surface offset'), to secure the position of the composite plate. The three different energy levels used in the experimental procedure were achieved by altering the initial velocity of the rigid impactor.

G1157/RTM-6 Interface Energy Release Rates	**Normal Energy Release Rate** G_{Ic} [kJ/m^2]		**Shear Energy Release Rate** G_{IIc} [kJ/m^2]
	0.18		0.5
G1157/RTM-6 Interface Damage Parameters	**Normal Failure Stress** $\sigma_{n,crit}$ [MPa]	**Shear Failure Stress** $\sigma_{s,crit}$ [MPa]	**Critical Distance** δ_{crit} [mm]
	8.13	22.59	0.04427

Table 2: Interface properties and damage parameters

3.3 Comparison of numerical and experimental results

The numerical results of the stacked shell finite element model for the case of the laminated plate subjected to low velocity impact are presented in comparison with the experimental results of [20]. The force versus time and force versus displacement curves calculated by the

stacked shell simulation for the three different energy levels are presented in Figure 4. It can be observed that the maximum load values predicted by the FE model are in good correlation to the experimental results, as the deviation is within 1% for the 6 J energy level, within 1.5% for the 10 J case, and only for the 13 J energy level deviation is increased to about 15%.

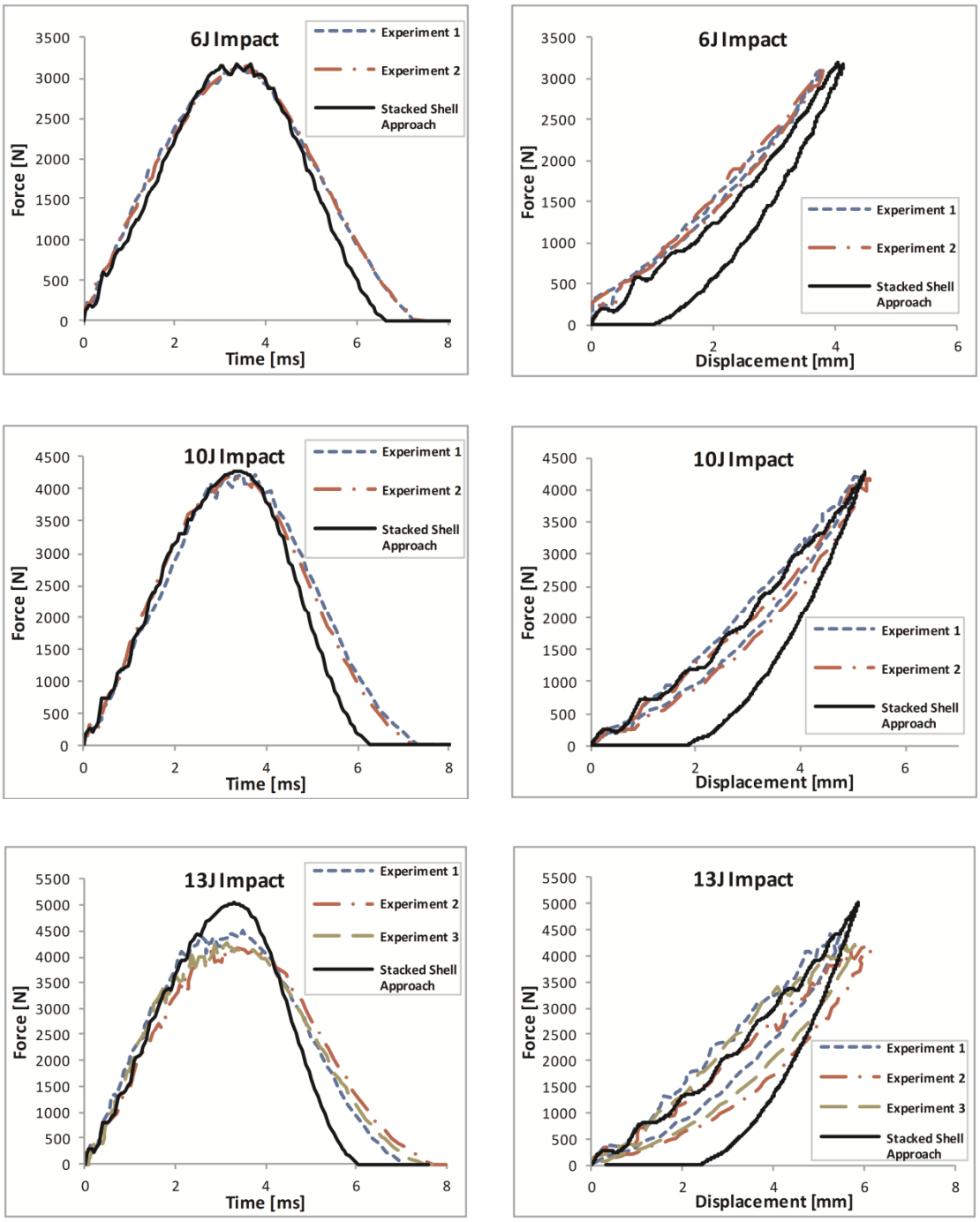

Figure 4: Comparison of simulation force-time and force-displacement curves with experimental results for 6 J, 10 J and 13 J energy levels

As far as the force versus displacement diagrams are concerned, excellent correlation to the experimental data can be observed for the loading phase, for all cases. The maximum displacement prediction is in excellent agreement with the experimental results. The deviation is ~8% for the 6J case, ~2% for the 10 J case and ~4% for the 13 J case. During the unloading

phase, the load capability tends to be underpredicted, a fact that can be attributed to a slight overprediction of the damage induced in plies.

Energy Level	Dimension [mm]	Thermography	Ultrasonic A-scan	Ultrasonic C-scan	Stacked Shell Approach
6 J	**Length**	14	20	20	**25**
	Width	7	15	14	**18**
10 J	**Length**	29	30	33	**32**
	Width	11	10	17	**19**
13 J	**Length**	41	40	42	**35**
	Width	18	22	20	**21**

Table 3: FE results for the delamination envelope dimensions compared to the experimental results of [20]

Stacked shell model predictions for the dimensions of the delamination envelope under the impacted area compared to results derived from NDT techniques are shown in Table 3. FE results correlate well with the experimental results, although for the lowest energy level, the delamination is slightly overestimated. Delamination plots of the seven contact interfaces are demonstrated in Figure 5, where the red color indicates delamination. As has also been reported by Abrate [15], it can be observed that at interfaces where adjacent plies have the same fiber orientation, almost no separation of plies occurs while, at points where damage is more intense delamination areas present an elongated 'peanut' shape, with the large dimension of the area oriented in the direction of the fibers of the lower ply that participates to the interface.

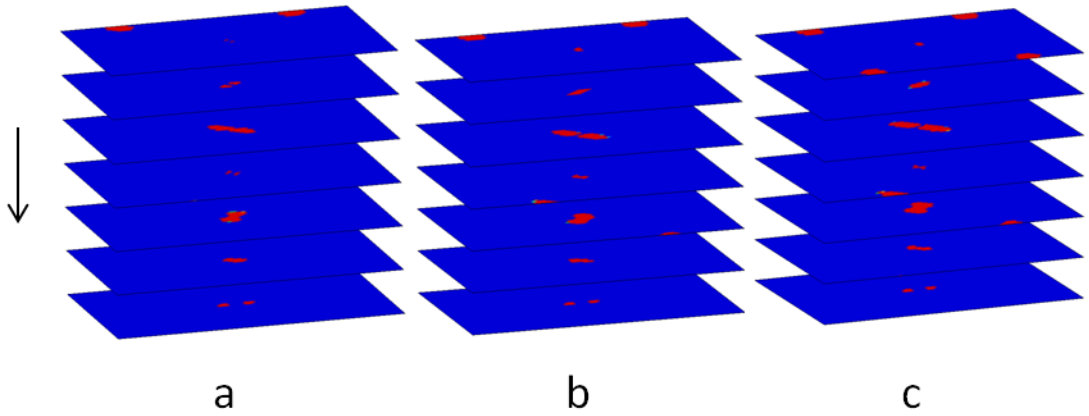

Figure 5: Delamination failure at interfaces. (a) 6 J, (b) 10 J, (c) 13 J

4 CONCLUSIONS

The stacked shell modeling methodology has been investigated in terms of explicit dynamics simulation of low velocity impact on fiber reinforced structures. The capabilities of the approach have been examined, with emphasis on the prediction of interlaminar damage. The investigation of the method's accuracy involves comparison with published experimental results concerning low speed impact on G1157/RTM-6 laminated plates. The stacked shell simulation results provide good correlation to the experimental results, as far as force and displacement predictions are concerned. The method's predictions of interlaminar failure (de-

lamination) present good agreement to the NDT derived experimental results. The good delamination prediction capabilities complimented by the method computational efficiency indicate that the stacked shell approach is a highly capable tool for the prediction of composite laminate behavior under low velocity impact conditions.

REFERENCES

[1] O. Allix and P. Ladevèze, Interlaminar interface modelling for the prediction of delamination. *Composite Structures*, **22**, 235-242, 1992.

[2] L. Daudeville and P. Ladevèze, A damage mechanics tool for laminate delamination. *Composite Structures*, **25**, 547-555, 1993.

[3] S. P. Rajbhandari, *Parametric finite element modeling of monolithic composite structures for impact damage*. Master of Engineering thesis, Royal Melbourne Institute of Technology, Australia, 2003.

[4] S. Sridharan, *Delamination behavior of composites*. Woodhead Publishing Limited, 2008.

[5] E. Rybicki and M. Kanninen, A finite element calculation of stress intensity factors by a modified crack closure integral. *Engineering Fracture Mechanics*, **09**, 931-938, 1977.

[6] D. Dugdale, Yielding of steel sheets containing slits. *Journal of the Mechanics and Physics of Solids*, **08**, 100-104, 1960.

[7] G. I. Barenblatt, The mathematical theory of equilibrium in brittle fracture. *Advances in Applied Mechanics*, **07**, 55–129, 1962.

[8] L. Greve and A. Pickett, Delamination testing and modelling for composite crash simulation. *Composites Science and Technology*, **66**, 816-826, 2006.

[9] S. Heimbs, S. Heller, P. Middendorf, F. Hähnel and J. Weiße, Low velocity impact on CFRP plates with compressive preload: Test and modeling. *International Journal of Impact Engineering*, **36**, 1182-1193, 2009.

[10] A. Johnson and M. David, Failure Mechanisms and Energy Absorption in Composite Elements under Axial Crush. *KEM*, **488-489**, 638-641, 2011.

[11] G. Pearce, A. Johnson, A. Hellier and R. Thomson, A Stacked-Shell Finite Element Approach for Modelling a Dynamically Loaded Composite Bolted Joint Under in-Plane Bearing Loads. *Applied Composite Materials*, **20**, 1025-1039, 2013.

[12] G. Pearce, A. Johnson, A. Hellier and R. Thomson, A study of dynamic pull-through failure of composite bolted joints using the stacked-shell finite element approach. *Composite Structures*, **118**, 86-93, 2014.

[13] B. Bussadori, K. Schuffenhauer and A. Scattina, Modelling of CFRP crushing structures in explicit crash analysis. *Composites Part B: Engineering*, **60**, 725-735, 2014.

[14] G. Lampeas and K. Fotopoulos, Interlaminar Stresses Calculation Using a Stacked-Shell Finite Element Modeling Approach. *International Journal of Applied Mechanics*, **07**, 1550067, 2015.

[15] S. Abrate, *Impact on composite structures.* Cambridge University Press, 1998.

[16] P. Maimi, J. Mayugo and P. Camanho, A Three-dimensional Damage Model for Transversely Isotropic Composite Laminates. *Journal of Composite Materials*, **42**, 2717-2745, 2008.

[17] Z. P. Bazant, B. H. Oh, Crack band theory for fracture of concrete. *Materials and structures*, **16**, 155-177, 1983.

[18] R. Borg, *Simulation of delamination initiation and growth in fiber composite laminates.* PhD Thesis, Linköpings universitet, Sweden, 2002.

[19] A. Turon, C. Dávila, P. Camanho and J. Costa, An engineering solution for mesh size effects in the simulation of delamination using cohesive zone models. *Engineering Fracture Mechanics*, **74**, 1665-1682, 2007.

[20] A. Riccio, F. Caputo, G. Di Felice, S. Saputo, C. Toscano and V. Lopresto, A Joint Numerical-Experimental Study on Impact Induced Intra-laminar and Inter-laminar Damage in Laminated Composites, *Applied Composite Materials*, 1-19, 2015, doi:10.1007/s10443-015-9457-0.

[21] E. Dvorkin and K. Bathe, A continuum mechanics based four-node shell element for general non-linear analysis. *Engineering Computations*, **01**, 77-88, 1984.

[22] J. O. Hallquist, *LS-DYNA Theory Manual.* Livermore Software Technology Corporation, 2015.

[23] A. Dobyns, Analysis of Simply-Supported Orthotropic Plates Subject to Static and Dynamic Loads. *AIAA Journal*, **19,** 642-650, 1981.